DOI: 10.1534/genetics.110.117200

Deletion of a Novel F-Box Protein, MUS-10, in *Neurospora crassa* Leads to Altered Mitochondrial Morphology, Instability of mtDNA and Senescence

Akihiro Kato,*[,1] Kiminori Kurashima,* Michael Chae,* Satoshi Sawada,* Shin Hatakeyama,*[,†,‡,2] Shuuitsu Tanaka* and Hirokazu Inoue*

**Laboratory of Genetics, Department of Regulatory Biology, Faculty of Science, †Molecular Analysis and Life Science Center and ‡Institute for Environmental Science and Technology, Saitama University, Saitama 338-8570, Japan*

Manuscript received April 1, 2010
Accepted for publication May 28, 2010

ABSTRACT

While mitochondria are renowned for their role in energy production, they also perform several other integral functions within the cell. Thus, it is not surprising that mitochondrial dysfunction can negatively impact cell viability. Although mitochondria have received an increasing amount of attention in recent years, there is still relatively little information about how proper maintenance of mitochondria and its genomes is achieved. The *Neurospora crassa mus-10* mutant was first identified through its increased sensitivity to methyl methanesulfonate (MMS) and was thus believed to be defective in some aspect of DNA repair. Here, we report that *mus-10* harbors fragmented mitochondria and that it accumulates deletions in its mitochondrial DNA (mtDNA), suggesting that the *mus-10* gene product is involved in mitochondrial maintenance. Interestingly, *mus-10* begins to senesce shortly after deletions are visualized in its mtDNA. To uncover the function of MUS-10, we used a gene rescue approach to clone the *mus-10* gene and discovered that it encodes a novel F-box protein. We show that MUS-10 interacts with a core component of the Skp, Cullin, F-box containing (SCF) complex, SCON-3, and that its F-box domain is essential for its function *in vivo*. Thus, we provide evidence that MUS-10 is part of an E3 ubiquitin ligase complex involved in maintaining the integrity of mitochondria and may function to prevent cellular senescence.

THE *mus-10* mutant was isolated from a screen aimed at identifying *Neurospora crassa* strains that were sensitive to MMS and therefore likely to lack proper DNA repair mechanisms (Kafer and Perlmutter 1980). Epistasis analyses involving *mus-10* suggested that it belonged to the *uvs-6* epistasis group, which functions in recombination repair (Kafer and Perlmutter 1980; Kafer 1983). However, *mus-10* did not display several phenotypes common to other members of the *uvs-6* epistasis group: chromosomal instability, a high sensitivity to histidine, and the inability to produce viable ascospores in homozygous crosses (Newmeyer *et al.* 1978; Newmeyer and Galeazzi 1978; Kafer and Perlmutter 1980; Kafer 1981; Schroeder 1986; Watanabe *et al.* 1997; Handa *et al.* 2000; Sakuraba *et al.* 2000). Furthermore, the frequencies of spontaneous and radiation-induced mutation observed in *mus-10* were similar to those of a wild-type strain (Kafer 1981). Past efforts to uncover the nature of these discrepancies or the function of the *mus-10* gene product have been uninformative.

The majority of cellular ATP is produced in mitochondria through aerobic respiration, which couples electron flow through respiratory complexes within the mitochondrial inner membrane with oxidative phosphorylation. Besides their role in ATP synthesis, mitochondria are also involved in many other cellular processes including beta-oxidation (Bartlett and Eaton 2004), calcium homeostasis (Gunter *et al.* 2004; Rimessi *et al.* 2008), production of iron-sulfur clusters (Zheng *et al.* 1998; Gerber and Lill 2002; Lill and Muhlenhoff 2005; Rouault and Tong 2005), and apoptosis (Green 2005; Antignani and Youle 2006; Xu and Shi 2007). Although virtually all mitochondrial proteins are encoded within the nucleus, a small number of proteins are encoded by mitochondrial DNA (mtDNA). The integrity of the mitochondrial genome may affect cell survival as mutations in mtDNA accumulate in patients suffering from severe neurological diseases including Alzheimer's, Huntington's and Parkinson's, as well as several types of cancer (Chatterjee *et al.* 2006; Higuchi 2007; Krishnan *et al.* 2007; Reeve *et al.* 2008). The number of mtDNA mutations also increases with age, suggesting a link between mitochondrial dysfunction and ageing (Cortopassi and Arnheim 1990; Corral-Debrinski

Sequence data from this article have been deposited with the DDBJ database under accession no. AB495263.

[1]*Present address:* Radiation Biology Center, Kyoto University, Kyoto 606-8501, Japan.

[2]*Corresponding author:* Laboratory of Genetics, Department of Regulatory Biology, Faculty of Science, Saitama University, Saitama 338-8570, Japan. E-mail: shinh@mail.saitama-u.ac.jp

et al. 1992; Cortopassi *et al.* 1992; Simonetti *et al.* 1992; Reeve *et al.* 2008). Contrary to the single genome in the nucleus, there are several copies of mtDNA in each mitochondrion. Thus, defects in a few mitochondrial genomes do not necessarily lead to mitochondrial dysfunction. Many patients suffering from mitochondrial diseases exhibit heteroplasmy, a phenomenon in which a mixture of wild-type and mutant mtDNAs exist in a single cell. The ratio of wild-type to mutant mtDNAs is critical in determining the penetrance of the genetic defect, where mutant loads >60% are required to cause respiratory chain dysfunction within an individual cell (Boulet *et al.* 1992; Chomyn *et al.* 1992; Sciacco *et al.* 1994).

Even though *N. crassa* strains are generally deemed immortal if they can be subcultured ~50 times, a wild-type strain was recently reported to senesce after 12,000 hr of growth, implying that this fungus undergoes natural or programmed ageing (Maheshwari and Navaraj 2008; Kothe *et al.* 2010). However, replicative life span is also influenced by genetic background as certain mutations can cause progressive deterioration of growth, ultimately leading to death. One such example is the nuclear-encoded *natural death* (*nd*), which when mutant causes a senescence phenotype correlating with the accumulation of multiple mtDNA deletions (Sheng 1951; Seidel-Rogol *et al.* 1989). The deletions of mtDNA in *nd* occurred between two 70- to 701-bp direct repeats, suggesting that the *nd* gene product regulates recombination, repair, or replication of mtDNA (Bertrand *et al.* 1993). Another nuclear mutation, *senescence* (*sen*), was isolated from *N. intermedia* and introgressed into *N. crassa* (Navaraj *et al.* 2000). Deletions were also observed in the mtDNA of *sen* mutants, but unlike those occurring in *nd* were flanked by 6- to 10-bp repeats typically associated with GC-rich palindromic sequences (D'Souza *et al.* 2005). The nature of the sequences that flanked the mtDNA deletions in these two mutants supported the existence of two distinct systems of mtDNA recombination in *N. crassa*: a general system of homologous recombination (system I) and a site-specific mechanism (system II), mediated in part by *nd* and *sen*, respectively (Bertrand *et al.* 1993; D'Souza *et al.* 2005). The *nd* and *sen* mutations have been mapped to linkage groups I and V, respectively, but neither gene has been cloned and the precise function of their gene products remains unclear. Two ultraviolet (UV)-sensitive mutants, *uvs-4* and *uvs-5*, are thought to undergo senescence, but unfortunately, these strains have not been studied in great detail (Schroeder 1970; Perkins *et al.* 1993; Hausner *et al.* 2006). Premature senescence has also been observed in cytoplasmic mutants of *N. crassa* including the E35 and ER-3 stopper mutants that harbor large mtDNA deletions, as well as strains that accumulate mitochondrial plasmids capable of inserting into mtDNA through homologous recombination (de Vries *et al.* 1986; Akins *et al.* 1989; Myers *et al.* 1989; Niagro and Mishra 1989; Court *et al.* 1991; Alves and Videira 1998).

While trying to establish the role of MUS-10 in DNA repair, we discovered that the *mus-10* mutant exhibited a shortened life span, an abnormal mitochondrial morphology and mtDNA instability. We cloned the *mus-10* gene through its ability to complement the MMS sensitivity of the *mus-10* mutant and revealed that it encoded a novel F-box protein. This suggested that MUS-10 is part of an Skp, Cullin, F-box containing (SCF) E3 ubiquitin ligase complex that targets proteins for degradation by the 26S proteasome. The data we present in this article offer proof that an SCF complex can regulate both mitochondrial maintenance and cellular senescence.

MATERIALS AND METHODS

Neurospora strains and cosmid libraries: The *N. crassa* strains used in this study are listed in Table 1. Growth and handling of *N. crassa* were performed as previously described (Davis and de Serres 1970). Some Neurospora strains, as well as the pMOcosX (Orbach 1994) and pLORIST (Kelkar *et al.* 2001) cosmid libraries were obtained from the Fungal Genetics Stock Center (FGSC; University of Missouri, Kansas City, MO). The original *mus-10* mutant (FGSC 5148) was twice backcrossed to C1-T10-28a to produce two *mus-10* isolates, KB27(10)-13A and KB27(10)-18a. Age-matched wild-type and *mus-10* mutant strains, K-byWT and K-byM10A, respectively, were obtained from a cross between KB27(10)-18a and 74-OR31-16A. A *mus-10* knockout strain, KTO-m10H2-1, was generated using a *mus-52* mutant (FGSC 9719) and standard protocols (Ninomiya *et al.* 2004). Removal of *mus-52*::*Bar* from KTO-m10H2-1 was achieved through a cross with C1-T10-34A producing KTO-10H-10A. To facilitate targeted integration at the *his-3* locus, KTO-10H-10A was crossed to a *his-3* mutant (FGSC 6103) to create the *mus-10 his-3* double mutant KRA-m10his3-5.

Measurement of linear growth and life span: Apical growth of hyphae was measured in race tubes that were ~30 cm in length (Ryan *et al.* 1943). Race tubes containing Vogel's minimal agar medium with 0.5 or 1.2% sucrose were inoculated with conidia at one end of the tube and incubated at 25° with constant light. The position of the growth front was marked once or twice a day to facilitate measurement of the apical growth rate. When hyphae reached the opposite side of the tube, a small piece of mycelia-containing medium was transferred to a fresh tube. To measure apical growth rates over an extended period of time, the entire process was repeated several times. Strains that were unable to traverse the race tube after numerous transfers to new medium were deemed to have a shortened life span.

Spot test analysis: The MMS sensitivity of various *N. crassa* strains was examined through spot tests. Briefly, conidia were harvested and washed twice with sterile water. The concentration of each conidial suspension was adjusted to 1×10^6 conidia/ml. These mixtures were then subjected to five 1:4 dilutions. A 10-μl aliquot of each suspension was spotted onto agar plates containing Vogel's minimal medium and sorbose. When required, MMS (0.015%) was added to the medium. Plates were incubated at 30° for 2 days and then photographed.

Isolation of mtDNA: Sucrose gradient-purified mitochondria were isolated from mycelia using previously described methods (Lambowitz 1979; Seidel-Rogol *et al.* 1989;

TABLE 1

***N. crassa* strains used in this study**

Strain	Genotype	Origin, source, or reference
C1-T10-28a	*a*	Tamaru and Inoue (1989)
C1-T10-34A	*A*	Tamaru and Inoue (1989)
C1-T10-37A	*A*	Tamaru and Inoue (1989)
74-OR31-16A	*A al-2 pan-2 cot-1*	de Serres (1980)
FGSC 5148	*A mus-10*	FGSC[a]
KB27(10)-13A	*A mus-10*	This study
KB27(10)-18a	*a mus-10*	This study
K-byWT	Undetermined	This study
K-byM10A	*A mus-10 pan-2*	This study
FGSC 9719	*a mus52::Bar*	FGSC
KTO-m10H2-1	*a mus-10::Hyg^r mus52::Bar*	This study
KTO-10H-10A	*A mus-10::Hyg^r*	This study
FGSC 6103	*A his-3*	FGSC
KRA-m10his3-5	*mus-10::Hyg^r his-3*	This study
KRA-m10M10F-2	*mus-10::Hyg^r his-3$^+$:mus-10-FLAG*	This study
KRA-m10dFM10F-1	*mus-10::Hyg^r his-3$^+$:mus-10$^{\Delta F\text{-}box}$-FLAG*	This study

[a] Fungal Genetics Stock Center, University of Missouri, Kansas City, MO, 64110.

Rowley *et al.* 1994). TE200 (200 mm Tris-HCl pH 8.0, 1 mm EDTA) was mixed with the mitochondria and then centrifuged at 15,000 rpm for 15 min. The mitochondrial pellet was resuspended in 250 μl of TE200, 40 μl of 20% SDS, and 290 μl of phenol:chloroform (1:1). After vigorous mixing, the sample was centrifuged at 12,000 rpm for 10 min. The aqueous phase was extracted two more times, first with phenol:chloroform and then with chloroform alone. The mtDNA was precipitated from the aqueous phase with ethanol, dissolved in TE buffer containing RNase A and then stored at −25°.

Cloning and sequencing of *mus-10* mtDNA: *Apa*I digestion of mtDNA obtained from the fifth subculture of *mus-10* generated a 6.6-kbp fragment that was extracted from an agarose gel and cloned into pBluescript SK$^+$ (Stratagene) to produce pmt*Apa*I. To identify the deletion breakpoints, smaller regions of the 6.6-kbp *Apa*I insert were sequentially subcloned into pBluescript using *Xba*I and then *Hin*dIII, generating pmt*Xba*I and pmt*Hin*dIII, respectively. The ends of all three inserts were sequenced using the universal T3 and T7 promoter primers and a BigDye sequencing kit (Applied Biosystems). Sequencing samples were run on an ABI PRISM 3100 genetic analyzer (Applied Biosystems). The sequences obtained in this manner were compared with mtDNA sequences from the Neurospora database (Assembly 3; Galagan *et al.* 2003).

Mitochondrial staining: Plates containing Vogel's minimal medium, 1.2% sucrose and 2% agar were inoculated with conidia and incubated overnight at 30°. To observe mitochondria in live cells, mycelia were stained with MitoFluor Red (Molecular Probes) or MitoTracker Green FM (Invitrogen). After 20 min at room temperature, a piece of mycelia-containing medium was transferred to a glass slide and examined by fluorescence microscopy. Mitochondria stained with MitoFluor Red were observed using a BX60 microscope (Olympus) and images were captured with a black-and-white camera (C4742-95; Hamamatsu). When MitoTracker Green FM was used, mitochondria were visualized and photographed using a confocal laser-scanning microscope (FV1000-D; Olympus).

Transformation of Neurospora: Neurospora transformations were performed as described with slight modifications (Ninomiya *et al.* 2004). Briefly, the conidial suspension was washed with 1 m sorbitol three times after which the concentration was adjusted to 2×10^9 conidia/ml. Linearized DNA (1–5 μg) was added to 100 μl of the conidial suspension and incubated on ice for 5 min. An aliquot of 40 μl was then transferred to a chilled electroporation cuvette (2 mm width). Electroporation was performed using a BTX Electro Cell Manipulation 600 (Genetronics) set at 1.5 kV and 186 ohm. After electroporation, the suspension was quickly removed from the cuvette and mixed with 960 μl of Vogel's minimal medium containing 1.2% sucrose. The conidia were incubated at 30° for 3 hr, mixed with molten top agar, and then spread over a selection medium. For the transformations that facilitated cloning of the *mus-10* gene, hygromycin B was used at a concentration of 500 μg/ml.

Cloning of *mus-10*: A 1.4-kbp *Sal*I fragment of pCB1003 (Carroll *et al.* 1994) containing the *Escherichia coli hph* gene controlled by the *Aspergillus nidulans trpC* gene promoter was subcloned into pBluescript SK$^+$ to produce pHS. *Not*I digestion of a pLORIST cosmid, H013 B4, generated an 8.5-kbp fragment that was cloned into the corresponding site of pHS to produce the plasmid pH 13-N8. A portion of pH 13-N8 was removed by *Sac*II digestion and subsequent recircularization with T4 DNA ligase to create the plasmid pH 13-SS. This plasmid included 3.1 kbp of sequence from H013 B4 and contained a single open reading frame, NCU02379.3, which was later confirmed as the *mus-10* gene.

MUS-10 antibody production: The 1.9-kb *mus-10* open reading frame (ORF) was amplified through PCR using a cDNA template and the primers MUS10-Ab-F (5′-GTACCA TATGACGTCCTCCTCCTCACTGGA-3′) and MUS10-Ab-R (5′-TACGAAGCTTGTCGTCGGGGTACGATTCCT-3′). This fragment was cloned into pET-21a (Novagen) using *Nde*I and *Hin*dIII restriction sites added by the primers used for PCR amplification. The resulting plasmid, pmus10-Ab-4, was transformed into Rosetta 2(DE3)pLysS *E.coli* competent cells (Novagen) to produce RS2m4-1. Expression of full-length MUS-10 protein in *E. coli* was performed as per the manufacturer's instructions. The cells were harvested by centrifugation and stored at −20° until processed.

To facilitate purification of MUS-10 inclusion bodies, frozen cell pellets were thawed on ice prior to addition of 3 ml of resuspension buffer [50 mm Tris-HCl pH 8.5, 5 mm EDTA,

1 mM phenylmethanesulfonyl fluoride (PMSF)] per gram of cells. The cells were lysed by sonication (8 × 15 sec bursts; UR-200P, Tomy Seiko, Tokyo, Japan). The insoluble fraction was pelleted through centrifugation and resuspended in 1 ml of wash buffer (50 mM Tris-HCl pH 8.5, 5 mM EDTA, 1% sodium deoxycholate). This mixture was subjected to a second round of sonication and the insoluble matter was again collected by centrifugation. The pellet was resuspended in 1 ml deoxycholate (1%) and incubated at 37° overnight. Following a final round of sonication and centrifugation, solubilization buffer (3 M urea, 10 mM Tris-HCl pH 8.0) was used to solubilize the purified inclusion bodies to a final concentration of 0.4 mg/ml. This mixture was sent to the antibody manufacturer Japan Lamb (Hiroshima, Japan) where it was injected into rabbits to facilitate production of polyclonal antibodies.

Protein isolation and Western blot analysis: Liquid media were inoculated with various *N. crassa* strains to a final concentration of 1×10^6 conidia/ml and grown at 30° for 18 hr with vigorous shaking. When indicated, MMS (0.05%) was added to the culture after 16 hr of growth and harvested with the untreated cultures 2 hr later. Previously published protocols were used for the preparation of cytosolic and crude mitochondrial protein fractions (Chae and Nargang 2009), purification of mitochondria through sucrose gradients (Lambowitz 1979; Rowley *et al.* 1994), SDS–PAGE (Laemmli 1970), and Western blotting (Good and Crosby 1989). Western blot analysis was performed using the anti-MUS-10 antibody described above (1/400), as well as three commercially available mouse monoclonal antibodies: ANTI-FLAG M2 antibody (1/10,000; Sigma, F3165), anti-α-tubulin (1/200,000; Sigma, T6074), and anti-COX3 (1/30,000; Molecular Probes, A-6408). Goat anti-mouse and goat anti-rabbit IgG, HRP conjugated secondary antibodies (Promega) were used at concentrations of 1/10,000 and 1/3000, respectively.

Yeast two-hybrid analysis: Yeast two-hybrid experiments were performed according to the manufacturer's instructions (Matchmaker Two-hybrid System 2 and 3, Clontech). Briefly, the primers m10-1 (5′-CCATGGATATGACGTCCTCCTCC TCA-3′) and m10-2 (5′-GGATCCCTAGTCGTCGGGGTAC GA-3′) were employed in RT–PCR to amplify a full-length *mus-10* cDNA. The primers used in PCR introduced *Nco*I and *Bam*HI restriction sites used to clone the *mus-10* cDNA into pACT2 and pGBKT7, producing the plasmids pACT2-*mus-10* and pGBKT7-*mus-10*, respectively. The GAL4 activation domain is encoded in pACT2 while pGKBT7 contains the GAL4 DNA binding domain. The plasmids pACT2-*scon-3* and pAS2-*scon-3* were generated in a similar manner, but using the primers scon3U (5′-CCATGGAGATGGCGGAGAACGACG-3′) and scon3L (5′-GGATCCCTAACGGTCTTCCGCCCA-3′). For the latter construct, *scon-3* was fused to the GAL4 DNA binding domain of pAS2-1 rather than that of pGBKT7. Plasmids carrying the GAL4 activation domain were cotransformed into yeast (Y187) with one of several constructs encoding the GAL4 DNA binding domain. Transformants were spread over plates containing medium lacking tryptophan and leucine, which selected for plasmids derived from pGBKT7 (or pAS2-1) and pACT2, respectively. Colonies resulting after 3 days at 30° were subjected to a filter assay for detection of β-galactosidase activity using the protocol described by Clontech.

Generation of FLAG-tagged wild-type and F-box deficient MUS-10: Two primers, S40-LnFG5 (5′-ccctcgaggatccggta gtatggactacaaagaccatgacggtgattataaagatcatgacatt-3′) and S41-LnFG3 (5′-ttgggcccttacttgtcatcgtcatccttgtaatccttgtaatcaatgtcat gatctttataatca-3′), which contain 22-bp complementary sequences at their termini, were used in a PCR reaction in the absence of template DNA to produce a 3xFLAG tag. This fragment was digested with *Xho*I and *Apa*I and cloned into the corresponding sites of pMF272, thereby removing the GFP gene contained in this plasmid (Freitag *et al.* 2004). This plasmid was named pFLAGC. m10Fc-5 (5′-GCTCTAGAGAT GACGTCCTCCTCCTCACT-3′) and m10-272Fc-3 (5′-GGAT CCGTCGTCGGGGTACGATTCCTTA-3′) were used to amplify the full-length *mus-10* ORF (637 codons) from *mus-10* cDNA. This fragment was cloned into pFLAGC using *Xba*I and *Bam*HI restriction sites introduced by the primers. This cloning procedure placed the *mus-10* ORF under the control of the *ccg-1* gene promoter and placed a 3xFLAG tag on the C terminus of the MUS-10 protein. A similar procedure was used to insert a truncated form of the *mus-10* ORF (codons 54–637) into pFLAGC, but in this case, the cloning was achieved using a different forward primer, dF-m10Fc-5 (5′-TCTAGAA CATGTCGTTTACTTTCTGGGAGCCTG-3′). Both constructs were transformed into a *mus-10 his-3* double mutant, KRA-m10his3-5, using electroporation. Desired transformants were selected by their ability to grow on media lacking histidine as elements from pMF272 promote targeted integration and reversion at the *his-3* locus (Freitag *et al.* 2004). In this manner, two *N. crassa* transformants were recovered, KRA-m10M10F-2 and KRA-m10dFM10F-1, which produced a full-length and F-box-deficient MUS-10 protein, respectively.

RESULTS

The *mus-10* mutant has a shortened life span: During our analysis of *mus-10*, we noticed that the viability of its conidia decreased through successive subculturing. To confirm our suspicions, we compared the apical growth rate of a wild-type strain and a *mus-10* mutant using race tubes. To ensure the inocula in these experiments were of similar age, *mus-10* was backcrossed to wild type and the resulting ascospores were randomly isolated and cultured. These age-matched progeny were characterized as carrying wild-type or mutant *mus-10* alleles on the basis of their sensitivity to MMS. Conidia from these strains were then used to inoculate race tubes. The apical growth rate of the wild-type strain remained constant over all of the time points examined (Figure 1). Conversely, growth of *mus-10* began to deteriorate after ~200 hr and completely stopped after ~380 hr (Figure 1). These data verified that *mus-10* exhibited a senescence phenotype.

mtDNA deletions in the *mus-10* mutant: The *nd* and *sen* mutants of *N. crassa* suffer from a shortened life span that correlates with the accumulation of mtDNA rearrangements (Sheng 1951; Seidel-Rogol *et al.* 1989; Bertrand *et al.* 1993; Navaraj *et al.* 2000; D'Souza *et al.* 2005). To investigate whether mtDNA rearrangements became more prevalent in *mus-10* as it aged, we isolated mtDNAs from five sequential subcultures of age-matched wild type and *mus-10*. Samples of mtDNA were digested with *Eco*RI or *Kpn*I and the resulting fragments were resolved using agarose gel electrophoresis. The mtDNAs obtained from the first three subcultures of wild type and *mus-10* displayed virtually identical restriction digest patterns (Figure 2A). However, mtDNAs from the fourth and fifth subcultures of *mus-10* produced an altered banding pattern characterized by the disappearance of the 8.8-kbp and 3.7-kbp *Eco*RI frag-

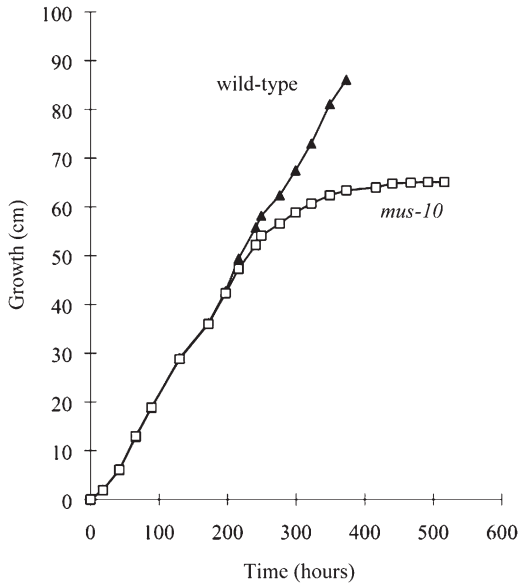

FIGURE 1.—Apical growth rates of wild-type and *mus-10* mutant strains. Conidia from age-matched wild-type (K-byWT) and *mus-10* (K-byM10A) were used to inoculate race tubes containing Vogel's minimal agar medium supplemented with 0.5% sucrose. Hyphal growth was recorded once or twice a day. Once the mycelia had traversed the tube, a piece of the growth front was transferred to a race tube containing fresh medium and the entire process was repeated. All race tubes were incubated at 25° under constant light.

ments (designated as *Eco*RI-3 and *Eco*RI-5, respectively; BERTRAND *et al.* 1993) and the emergence of a 4.4-kbp *Eco*RI band (Figure 2A). Similarly, the 21.6-kbp *Kpn*I fragment seemed to be replaced by a novel band of ~10 kbp (Figure 2A). No such changes were observed in age-matched wild-type strains. Unfortunately, the three smallest *Eco*RI fragments (*Eco*RI-8, -9 and -10) could not be clearly observed in our experiments, and thus we could not determine whether these bands were modified in any way. mtDNAs from older wild type and *mus-10* (fifth subculture) also produced differing restriction digest patterns when digested with *Apa*I and *Cla*I (Figure 2B). On the basis of these results, we estimated that the mtDNA of *mus-10* carried a 10- to12-kbp deletion (Figure 2C).

Cloning and analysis of *mus-10* mtDNA: To uncover the region of mtDNA deleted in *mus-10*, we first needed to determine the sequence of the flanking regions. We reasoned that the 6.6-kbp *Apa*I restriction fragment observed in mtDNA from the fifth subculture of *mus-10*, but absent in that of wild type, likely resulted from a large deletion involving the 12.9-kbp and possibly the 5.8-kbp *Apa*I fragments (Figure 2C). This novel *Apa*I band was cloned into the corresponding site of pBluescript. The ends of the 6.6-kbp insert were sequenced with the universal T7 and T3 promoter primers but unfortunately, no mtDNA deletions were detected in the sequenced region when compared with mtDNA sequences from the Neurospora database (assembly 3; GALAGAN *et al.* 2003). This implied that the deletion breakpoint occurred further into the cloned mtDNA fragment. Consequently, a 2.2-kbp region of mtDNA from the cloned *Apa*I restriction fragment was subcloned into pBluescript using *Xba*I. Sequence analysis was performed as described above, but the deletion breakpoints could not be identified. Subsequent sequencing of pmt*Hin*dIII, which contained 1.2 kbp of mtDNA obtained from digestion of the 6.6-kbp *Apa*I restriction fragment with *Hin*dIII, finally revealed a 10,488-bp deletion in the mtDNA of *mus-10*. This deletion completely removed *Eco*RI-3 as well as parts of *Eco*RI-5 and *Eco*RI-10, thereby eliminating two unidentified reading frames (*urfU* and *urfN*), *cox1* (cytochrome *c* oxidase subunit 1), *cob* (apocytochrome *b*), and part of *nad1* (NADH dehydrogenase subunit 1) (Figure 3A).

Further examination revealed that the deleted region was flanked by 7-bp direct repeats (AGGGGGG; Figure 3B), resembling sequences associated with system II, the site-specific mtDNA recombination pathway. Interestingly, the first four nucleotides of the 5′ repeat overlapped an 18-bp *Pst*I palindrome (5′-CCCTGCAG TACTGCAGGG-3′) that occurs in mtDNA of *N. crassa* 67 times (CAHAN and KENNELL 2005) and is thought to form a stem-loop structure (Figure 3C; YIN *et al.* 1981; NARGANG *et al.* 1983; DE VRIES *et al.* 1986).

Mitochondrial morphology of the *mus-10* mutant: Our restriction digest analysis of mtDNA suggested that loss of the *mus-10* gene had an adverse effect on mitochondria. To explore this hypothesis, we used fluorescence microscopy to examine the morphology of mitochondria within *mus-10*. Growing hyphae were stained with a mitochondria-specific fluorescent dye and then visualized under a microscope. In wild-type mycelia, long tubular mitochondria were observed in both distal and conidiating hyphae (Figure 4). Conversely, *mus-10* had abnormal mitochondria that exhibited a spherical morphology (Figure 4). Surprisingly, the occurrence of this phenotype was not age related, as spherical mitochondria were observed in earlier subcultures during which hyphae were growing normally (Figure 4). This implies that changes to mitochondrial structure occur prior to the formation of abnormal mtDNAs.

Identification of the *mus-10* gene: The *mus-10* gene was previously mapped to a site on LG VII near *met-7* (7%; KAFER and PERLMUTTER 1980). To identify the *mus-10* gene, we used a gene-rescue approach in which *mus-10* conidia were transformed with digested cosmids that spanned a 27.7-kbp region defined by our linkage and RFLP analyses (data not shown). In this manner, we discovered an 8.5-kbp *Not*I fragment derived from the pLORIST cosmid H013 B4 that could rescue the MMS sensitivity of *mus-10*. This fragment was cloned into pHS to produce pH 13-N8 (Figure 5). The sequence in this fragment contained three annotated ORFs: NCU02379.3, NCU02378.3, and NCU02377.3 (Figure 5). Removal of the latter two ORFs from pH 13-N8 was

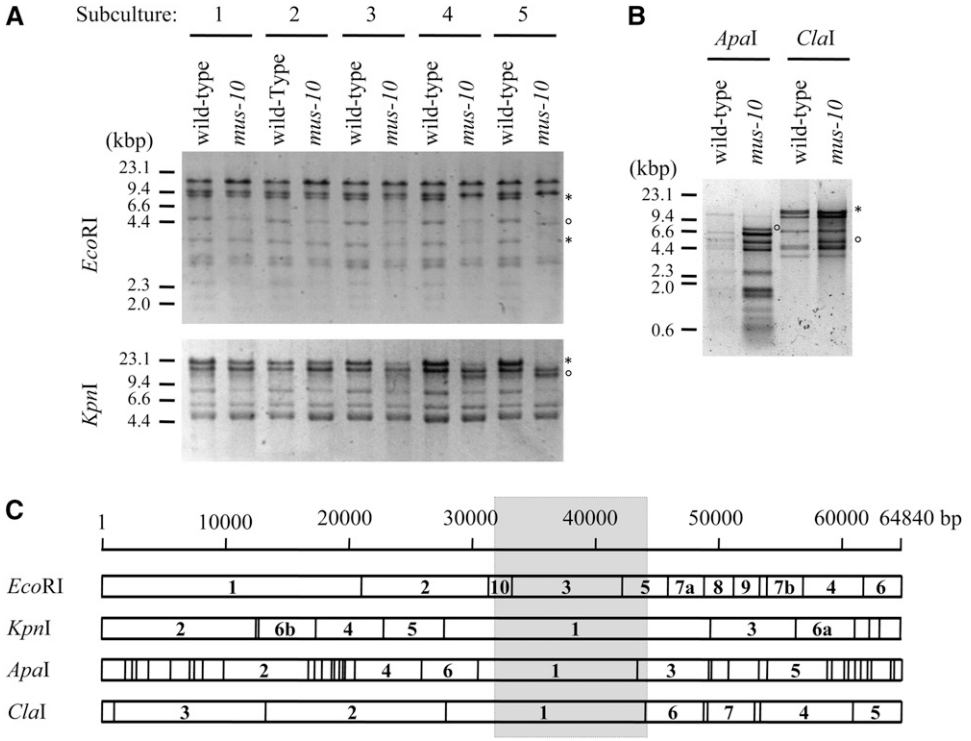

FIGURE 2.—Restriction analysis of mtDNA. (A) mtDNAs were isolated from five sequential subcultures (labeled 1–5) of wild-type and *mus-10* mutant strains. These mtDNAs were digested with *Eco*RI or *Kpn*I, and subjected to agarose gel electrophoresis. Bands emerging or disappearing in the fourth and fifth subcultures of *mus-10* are indicated with an open circle (°) and asterisk (*), respectively. (B) mtDNAs from the fifth subculture of wild-type and *mus-10* mutant strains were digested with *Apa*I or *Cla*I. Restriction digest fragments that differed between the two strains are indicated as described in A. (C) Restriction maps of *N. crassa* mtDNA digested with *Apa*I, *Cla*I, *Eco*RI, or *Kpn*I. Position 1 in this figure corresponds to the nucleotide at the 5′ end of the largest *Eco*RI fragment. Numbers located within the mtDNA fragments indicate their size relative to the other fragments generated from digestion with a given restriction enzyme. The number "1" is used to describe the largest fragment, while "a" and "b" are employed when two fragments of similar size are produced, where "a" specifies the larger fragment. The shaded area shows the predicted location of a large mtDNA deletion (~10–12 kbp) observed in latter cultures of *mus-10*.

achieved through *Sac*II digestion and subsequent recircularization of the desired fragment to generate the plasmid pH 13-SS. The 3.1-kbp insert in this plasmid contained a single ORF (NCU02379.3) that conferred wild-type MMS resistance to *mus-10*. To confirm the identity of the *mus-10* gene, we isolated genomic DNA from the original *mus-10* mutant and employed PCR to amplify the candidate gene. Sequence analysis of this PCR product revealed that *mus-10* carries a single G-to-A transition at position 984 of the predicted ORF sequence, producing a nonsense mutation (Figure 5).

The *mus-10* gene was predicted to encode a 637 residue polypeptide with a molecular weight of 73.7 kDa. The ORF sequence and intron–exon boundaries were confirmed through sequence analysis of cDNA generated through RT–PCR. An F-box was identified at the N terminus of the MUS-10 protein (Figure 5), suggesting that it belongs to the F-box protein family whose members are normally components of SCF E3 ubiquitin ligase complexes that direct proteins to the 26S proteasome, ultimately leading to their degradation. These findings are concurrent with the hypothesis that SCF complexes can regulate mitochondrial function (COHEN *et al.* 2008; DENG *et al.* 2008). A *YccV*-like domain, which has been shown to bind hemimethylated DNA (D'ALENCON *et al.* 2003), was also observed in MUS-10, suggesting that it may be capable of interacting with DNA (Figure 5).

Localization of MUS-10: To help elucidate the function of MUS-10, we wanted to establish its subcellular location. Western blot analysis was performed on cytosolic and purified mitochondrial proteins isolated from a wild-type strain (C1-T10-37A) and a *mus-10* knockout (KTO-10H-10A). To ensure the absence of cytosolic proteins in the mitochondrial fraction and vice versa, blots were also examined using antibodies against α-tubulin and COX3, which are found in cytosol and mitochondria, respectively (Figure 6). Use of an anti-MUS-10 antibody revealed a band in the cytosolic fraction of wild type that was absent in *mus-10* (Figure 6, lanes 1 and 3). Conversely, MUS-10 was not observed in mitochondria from either strain (Figure 6, lanes 5 and 7).

Since MUS-10 appears to influence mitochondrial morphology and also protects cells against the effects of MMS, we reasoned that exposure to MMS may induce movement of MUS-10 from the cytosol to mitochondria. However, MUS-10 localization was not altered in cells grown in the presence of MMS (Figure 6). Taken together, these results suggest that MUS-10 may function in the cytosol.

MUS-10 is part of an SCF complex: Proteins with an F-box motif (F-box proteins) generally function in SCF E3 ubiquitin ligase complexes along with two additional core components, Cullin and Skp1, although they are thought to physically interact only with the latter (BAI *et al.* 1996; JACKSON and ELDRIDGE 2002; WILLEMS *et al.*

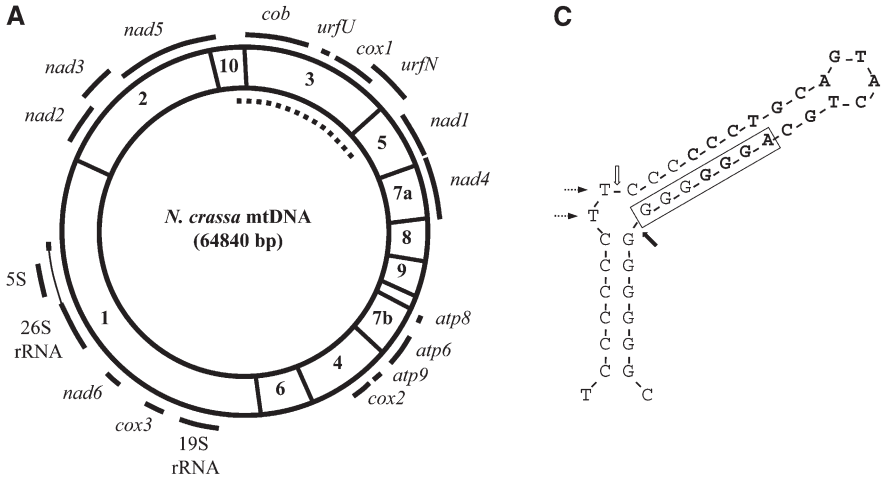

FIGURE 3.—Characterization of the mtDNA deletion observed in *mus-10*. (A) A circular *Eco*RI restriction map of *N. crassa* mtDNA. The sizes of the *Eco*RI fragments are indicated as described in Figure 2C. The location of genes and rRNAs are indicated with solid black lines. The dotted line denotes the mtDNA deleted in *mus-10*. (B) Location of the mtDNA deletion breakpoints of *mus-10*. The 10,488-bp deletion detected in *mus-10* was flanked by 7-bp direct repeats (indicated with boxes) present in *Eco*RI-10 and *Eco*RI-5. Numbers beside the mtDNA sequences indicate the position of nucleotides relative to the closest 5′ *Eco*RI restriction site. The recombining sequences that gave rise to the mtDNA observed in pmt*Hin*dIII are indicated with a solid line. The 18-bp *Pst*I palindrome associated with deletions of mtDNA in *mus-10* and *sen* is shown in boldface type. (C) Predicted stem-loop structure of the mtDNA sequence (nucleotides 1572–1610 of *Eco*RI-10) surrounding the 5′ deletion junction. The nucleotides that comprise the *Pst*I palindrome are shown in boldface type. The 7-bp direct repeat of *Eco*RI-10 is indicated with a box. The two unpaired thymine residues that are thought to trigger BER or MMR pathways are shown with dotted arrows. The positions where single strand breaks likely occurred to facilitate deletions of mtDNA in *mus-10* and *sen* are indicated with solid and open block arrows, respectively.

2004; Ho *et al.* 2008). To investigate whether MUS-10 physically interacts with SCON-3 (the Neurospora Skp1 homolog; SIZEMORE and PAIETTA 2002) a yeast two-hybrid assay was performed. cDNAs of *mus-10* and *scon-3* were cloned into yeast expression vectors containing the Gal4p activation or DNA binding domains. A filter assay showed that β-galactosidase was produced when yeast cells were cotransformed with constructs carrying *mus-10* and *scon-3* fused to the DNA binding and activation domains of Gal4p, respectively, while no β-galactosidase activity was observed in any of the control experiments (Figure 7A). Although fewer yeast colonies were generated in reciprocal experiments, β-galactosidase activity could still be detected (Figure 7B). These data are consistent with a physical interaction between MUS-10 and SCON-3.

The F-box motif of MUS-10 is required for its function: The F-box motif normally interacts with Skp1 and is thought to be essential for F-box protein function (BAI *et al.* 1996). To confirm the importance of the MUS-10 F-box motif, we examined whether a MUS-10 protein lacking the F-box motif could rescue the phenotypes of the *mus-10* mutant. Full-length and F-box-deficient versions of the *mus-10* gene were inserted into pFLAGC, which placed them under the control of the constitutive *ccg-1* gene promoter (FREITAG *et al.* 2004) and added a

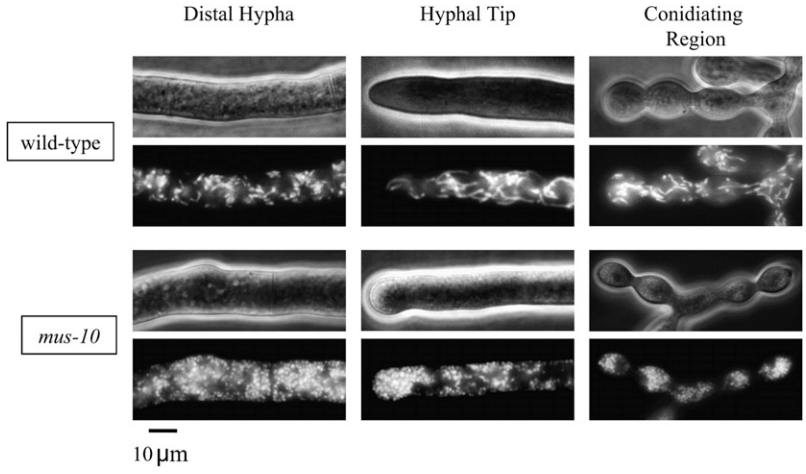

FIGURE 4.—The morphology of mitochondria in wild-type and *mus-10* mutant strains. Growing hyphae from the first subculture of wild-type (K-byWT) and *mus-10* (K-byM10A) strains were stained with MitoFluor Red and then visualized using fluorescence microscopy (lower). These hyphae were also observed using phase-contrast microscopy (upper).

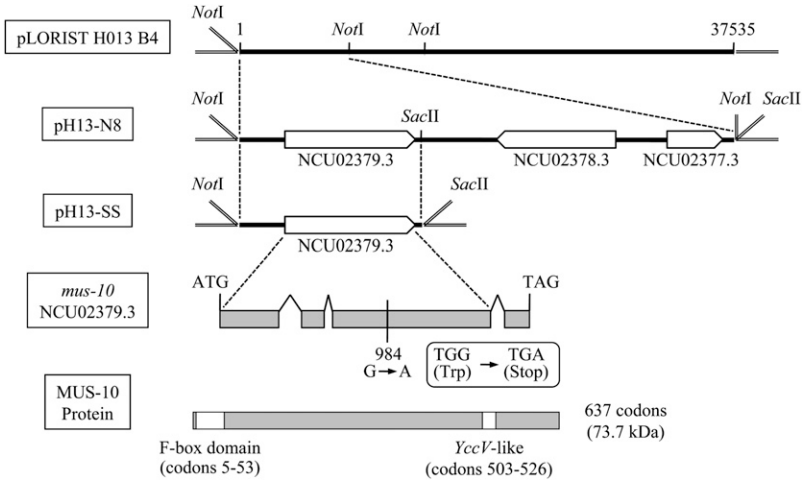

FIGURE 5.—Identification of the *mus-10* gene. *Not*I digestion of pLORIST H013 B4 produced an 8.5-kbp fragment that could restore growth of *mus-10* on medium containing MMS. This fragment was cloned into pHS to produce pH 13-N8. Sequence analysis of pH 13-N8 revealed three predicted ORFs, NCU02379.3, NCU02378.3, and NCU02377.3. To identify the *mus-10* gene, a portion of pH 13-N8 was removed with *Sac*II producing pH 13-SS. This plasmid contained a single ORF, NCU02379.3, and could complement the *mus-10* mutant phenotype. Sequencing revealed that the *mus-10* mutant carried a G-to-A transition at position 984 of this ORF, which generated a nonsense mutation. ORF NCU02379.3 is predicted to encode a 637-amino acid polypeptide with a molecular weight of 73.7 kDa. Analysis of the amino acid sequence revealed an F-box domain (codons 5–53) and a *YccV*-like domain (codons 503–526).

3xFLAG-tag to the C terminus of each protein (Figure 8A). Transformation of these constructs into a *mus-10* knockout produced strains that were revealed through Western blot analysis to contain relatively high levels of FLAG-tagged full-length or truncated MUS-10 protein within the cytosol (Figure 8B, lanes 2 and 3). Unfortunately, the anti-FLAG antibody also recognized a nonspecific protein similar in size to full-length MUS-10 (lanes 1 and 3). However, given the intensity of the band observed in *mus-10* transformed with the full-length construct (lane 2), it is clear that FLAG-tagged MUS-10 is being produced in this strain. Surprisingly, a small amount of full-length and ΔF-box-deficient MUS-10 were detected in mitochondria with the relative levels of the two proteins being similar to that observed in the cytoplasm (Figure 8B, lanes 2 and 3 *vs.* lanes 5 and 6). This may suggest that overexpression of the two MUS-10 forms leads to or increases their association with mitochondria. While this result will be addressed further in DISCUSSION, it is important to note that the ΔF-box MUS-10 was also observed in mitochondria and thus, removal of the first 53 amino acids did not remove an N-terminal mitochondrial signal sequence.

After we confirmed expression of both FLAG-tagged MUS-10 proteins, we performed spot test analysis to determine whether these proteins could rescue the MMS sensitivity of *mus-10*. As anticipated, strains expressing full-length MUS-10 protein displayed wild-type growth on MMS plates while those carrying the truncated form of MUS-10 lacking the F-box motif remained susceptible to MMS (Figure 9A).

To examine whether these transformants exhibited a shortened life span, their growth rates were monitored in race tubes. Transformants that expressed full-length MUS-10 displayed wild-type growth, while those harboring the F-box deficient form senescence prematurely (Figure 9B). Although the strain expressing the truncated form of MUS-10 appeared to undergo senescence earlier than the original *mus-10* mutant (Figure 9B), it should be noted that deficiencies leading to senescence likely continued to accumulate during the transformation procedure, and thus conidia from this transformant are likely "older" than those of the original *mus-10* mutant. Fluorescence microscopy revealed that tubular mitochondria could be restored in *mus-10* through transformation with a construct encoding wild-type, but not truncated, MUS-10 protein (Figure 9C). Taken together, these data confirm that the F-box domain of MUS-10 is essential for its function *in vivo*.

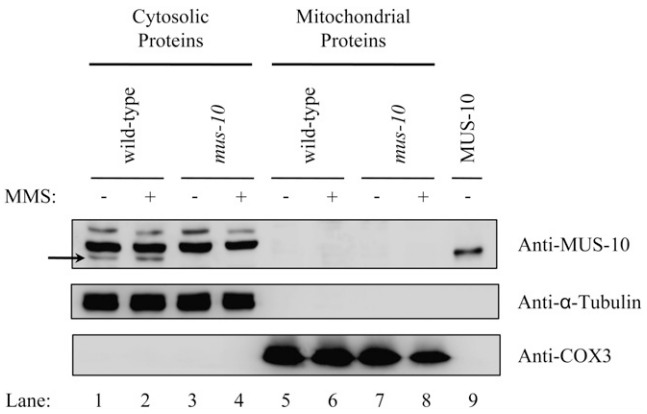

FIGURE 6.—MUS-10 localization. Western blot analysis was performed using cytosolic proteins (200 μg) and sucrose gradient-purified mitochondria (50 μg) isolated from a wild-type (C1-T10-37A) and *mus-10* mutant strain (KTO-10H-10A) grown in the presence (+) or absence (−) of MMS. Anti-α-tubulin and anti-COX3 were used as controls to identify cytosolic and mitochondrial marker proteins, respectively. A total of 250 ng of recombinant MUS-10 (MUS-10) was loaded in the gel to verify functionality of the MUS-10 antibody. Since use of the anti-MUS-10 antibody produced several nonspecific bands, the location of MUS-10 is indicated with a solid arrow.

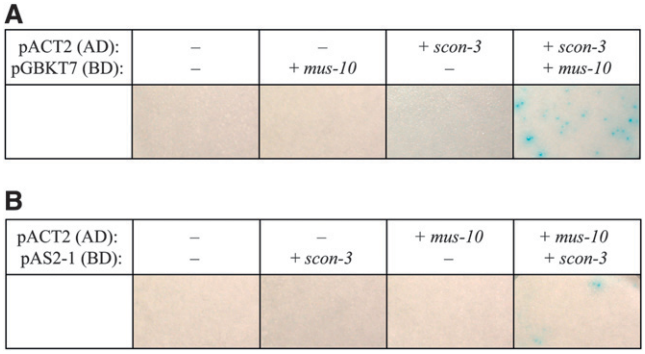

FIGURE 7.—A physical interaction between MUS-10 and SCON-3. Yeast two-hybrid analysis was performed to determine whether the MUS-10 protein interacted with a core component of *N. crassa* SCF complexes, SCON-3. (A) Yeast cells (Y187) were cotransformed with two plasmids, one of which contained the GAL4 activation domain (AD) of pACT2 while the other included a GAL4 DNA binding domain (BD) from pGBKT7. While empty vectors (−) were used in some of these experiments, transformations were also performed with derivatives of pACT2 and pGBKT7 that contained in-frame *scon-3* (+ *scon-3*) and *mus-10* (+ *mus-10*) cDNAs, respectively. Selection of cotransformants was achieved using nutritional markers present within pACT2 and pGBKT7, which confer the ability to grow on medium lacking leucine and tryptophan, respectively. Colonies emerging after a 3-day incubation at 30° were subjected to a filter assay capable of detecting β-galactosidase activity, which would only be observed if the two proteins being examined could physically interact. (B) Reciprocal experiments performed as described in A. In these experiments, pAS2-1, which contains the GAL4 DNA binding domain and the *TRP1* gene, was used in place of pGBKT7.

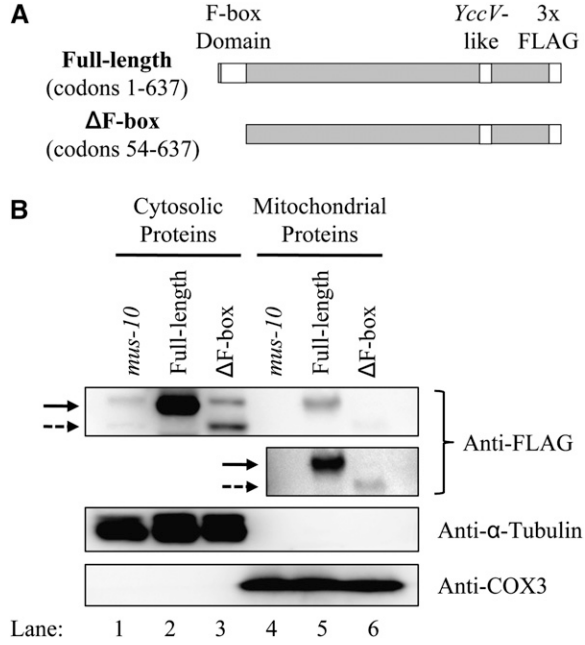

FIGURE 8.—FLAG-tagged forms of MUS-10. (A) Diagram of full-length (codons 1–637) and truncated (codons 54–637) MUS-10 used in our experiments. Insertion of cDNAs encoding the two forms of MUS-10 into pFLAGC placed their expression under the control of the constitutive *ccg-1* gene promoter and added a 3xFLAG tag on the C terminus of each protein. Since pFLAGC is derived from pMF272, it contains a portion of the *N. crassa his-3* gene, which can be used for targeted integration and reversion at the *his-3* locus. (B) Western blot analysis was performed as described in Figure 6. Plasmids encoding the two different FLAG-tagged versions of MUS-10 (shown in A) were used to transform *mus-10* (KRA-m10his3-5) conidia. Two resulting *his*$^+$ transformants, KRA-m10M10F-2 and KRA-m10dFM10F-1, expressed full-length and ΔF-box MUS-10, respectively. Background levels were determined using untransformed *mus-10*. Full-length MUS-10 protein is indicated with a solid arrow, while the ΔF-box form is shown with a dotted arrow. To facilitate viewing of MUS-10 in the mitochondrial fraction, a second, longer exposure was also included (Anti-FLAG, lower).

DISCUSSION

Although sensitivity of *mus-10* to MMS and UV light implied a deficiency in one or more DNA repair pathways, the precise function of the *mus-10* gene was unclear. In this present work we report that MUS-10 belongs to the F-box protein family and is thus likely involved in proteasome-mediated protein turnover. This finding suggests that even though *mus-10* is more susceptible to MMS than wild type, the *mus-10* gene product may not have a direct role in DNA repair. Indeed, other instances of this phenomenon have been reported in other organisms. In *S. cerevisiae*, an increased sensitivity to MMS was observed in strains deficient for Tim13p, whose role in mitochondrial protein import is well established (HANWAY *et al.* 2002). It was hypothesized that the heightened susceptibility of the *tim13*Δ strain to MMS resulted from the reduced import of mtDNA repair proteins. Conversely, overexpression of a nuclear BER protein in the mitochondria of human cells was thought to cause an imbalance of mitochondrial DNA repair proteins making them more vulnerable to MMS (FISHEL *et al.* 2003). Since MUS-10 is likely to function in ubiquitin-mediated proteolysis, it is conceivable that MUS-10 deficiency promotes accumulation of one or more mitochondrial proteins that affect mtDNA repair, replication, or recombination, leading to an elevated sensitivity to MMS.

Similar to *nd* and *sen*, strains deficient for *mus-10* displayed a shortened life span and accumulated mtDNA deletions (SEIDEL-ROGOL *et al.* 1989; BERTRAND *et al.* 1993; NAVARAJ *et al.* 2000; D'SOUZA *et al.* 2005). Analysis of the mtDNA deletion observed in latter subcultures of *mus-10* revealed the absence of *Eco*RI-3 and parts of *Eco*RI-5 and *Eco*RI-10. This deletion removed at least three components of the electron transport chain, *cob*, *cox1*, and *nad1*, which likely impaired respiration leading to senescence and subsequent death of *mus-10*. Similarly, the stop–start growth phenotype of the E35 stopper mutant was attributed to loss of *nad2* and *nad3* (DE VRIES *et al.* 1986; ALVES and VIDEIRA 1998), while the ER-3 stopper mutant was shown to harbor a ~25-kbp deletion of mtDNA that removed several genes including *cob* and *cox1* (NIAGRO and

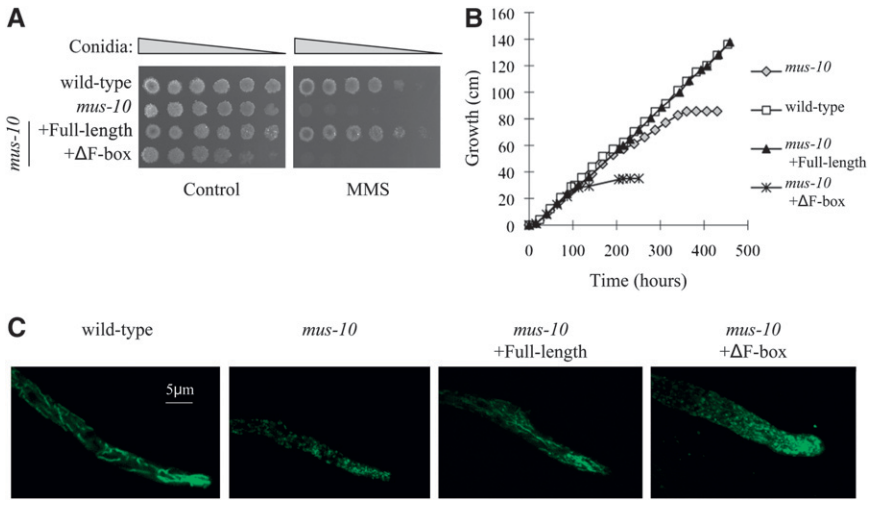

FIGURE 9.—The F-box of MUS-10 is essential for its function. (A) Spot test analysis was performed using conidia from C1-T10-37A (wild type), KTO-10H-10A (*mus-10*), KRA-m10M10F-2 (*mus-10* + full-length) and KRA-m10dFM10F-1 (*mus-10* + ΔF-box). Conidial suspensions were adjusted to a concentration of 1×10^6 conidia/ml and subjected to five 1:4 serial dilutions. A 10-μl aliquot of each mixture was spotted onto agar plates containing Vogels's minimal sorbose medium lacking (control) or supplemented with 0.015% MMS (MMS). Plates were photographed after 2 days at 30°. (B) Measurements of apical growth were performed as described in Figure 1. In these experiments, race tubes contained 1.2% sucrose instead of 0.5%. (C) Mitochondrial morphology. Live hyphae were stained with MitoTracker Green and visualized using a confocal laser-scanning microscope.

MISHRA 1989; NIAGRO and MISHRA 1990). Senescence in these and other *N. crassa* strains, including *nd*, *sen*, and *mus-10*, correlated with the accumulation of mtDNAs that harbor large deletions, which may incur a replicative advantage over wild-type molecules due to their smaller size. In a recent report, quantitative real-time PCR was used to demonstrate that in mice, mitochondrial genomes that contain large deletions (~10 kb) accumulated faster than those carrying small deletions (~3.8 kb) (FUKUI and MORAES 2009). While these data support the notion that smaller mtDNAs have a replicative advantage over larger ones, it does not exclude the possibility that the number and/or nature of the genes present in a mitochondrial genome can influence copy number.

The *Pst*I palindrome observed at the 5′ flank of the *mus-10* mtDNA deletion is capable of forming a GC-rich imperfect stem loop, a structure which has been hypothesized to stall DNA replication and/or act as substrates for mismatch repair (MMR) or base excision repair (BER) systems (D'SOUZA *et al.* 2005; HAUSNER *et al.* 2006). Either scenario could lead to single and/or double strand breaks that are thought to promote mtDNA recombination. Indeed, the stem-loop structure formed by the *Pst*I palindrome flanking the *mus-10* mtDNA deletion contains two unpaired nucleotides that could potentially trigger BER or MMR pathways resulting in endonucleolytic cleavage of the phosphodiester bond following the AGGGGGG repeat (Figure 3C). Interestingly, the same *Pst*I palindrome and unpaired nucleotides were implicated in the generation of mtDNA deletions in *sen* (recombination junction J2; D'SOUZA *et al.* 2005), but in this case, the cleavage event occurred on the opposite strand (Figure 3C), implying that mtDNA repair pathways can target either strand of the mismatched and/or unpaired sequence.

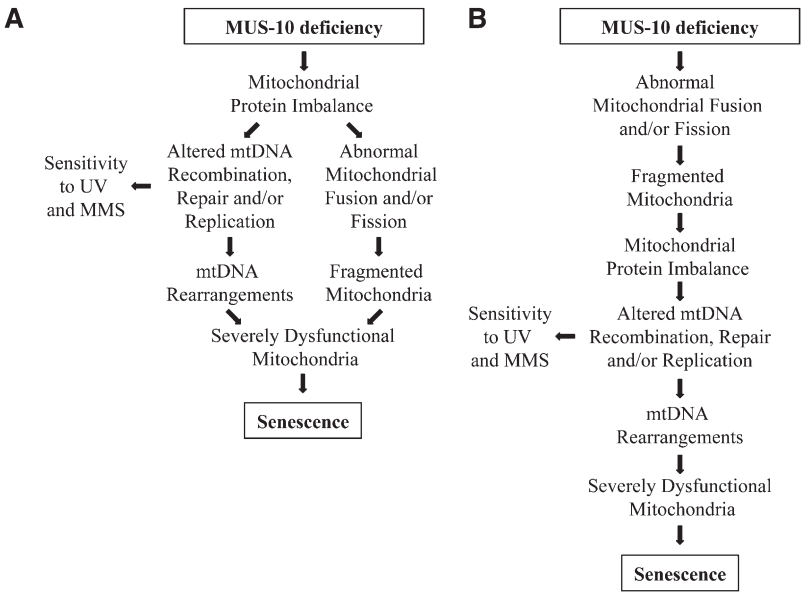

FIGURE 10.—Models to explain the relationship between *mus-10* and senescence. (A) In this model, loss of MUS-10 prevents operation of a mitochondrial E3 ubiquitin ligase leading to accumulation and/or deficiency of numerous mitochondrial proteins. The resulting protein imbalance leads to defects in both mtDNA maintenance and mitochondrial morphology through independent mechanisms. Defective mtDNA recombination, repair, and/or replication leads to increased MMS/UV-light sensitivity and mtDNA rearrangements. Mitochondrial fragmentation and altered mtDNA promote further mitochondrial dysfunction, which ultimately results in impaired respiration and eventual senescence. (B) This model is similar to the one proposed in A except that in this case, dysfunction of mtDNA recombination, repair, and/or replication results from a mitochondrial protein imbalance caused by mitochondrial fragmentation and is thus not a direct result of MUS-10 deficiency.

Our examination of mitochondrial morphology and mtDNA rearrangements in *mus-10* suggests that fragmented mitochondria arise prior to modification in the mtDNA restriction digest profile. While we cannot exclude the possibility that mtDNA rearrangements arise in *mus-10* much earlier than they can be visualized through restriction digest and agarose gel electrophoresis, our observations do raise the question of whether mitochondrial fragmentation leads to altered mtDNA or if these events occur through independent mechanisms. We propose two models that address the relationship between mitochondrial morphology and mtDNA integrity, both of which rely on MUS-10 functioning as an E3 ubiquitin ligase. In our first model (Figure 10A), MUS-10 deficiency is proposed to promote the accumulation of a wide variety of mitochondrial proteins including, but not limited to, mediators of fission and/or fusion, components of import machinery, and proteases. Accumulation of mitochondrial proteases would subsequently lead to lower levels of their substrates. The resulting mitochondrial protein imbalance has two concurrent effects: (i) deficiencies in mtDNA replication, recombination, and/or repair, leading to mtDNA rearrangements and sensitivity to MMS and UV, and (ii) disruption of the fission/fusion equilibrium, resulting in mitochondrial fragmentation. The persistence of such problems promotes further mitochondrial defects, which initiates a vicious cycle leading to the accumulation of dysfunctional mitochondria that ultimately cause senescence. Our second model (Figure 10B) proposes that loss of MUS-10 leads to the production of fragmented mitochondria through inhibited mitochondrial fusion and/or accelerated division. This model predicts that smaller mitochondria are more likely to harbor an imbalanced protein complement and are thus prone to defective maintenance of mtDNA. This compromises respiration, which in turn leads to senescence.

Regardless of whether there is a causal relationship between defective mtDNA and mitochondrial morphology in *mus-10*, the fragmented mitochondria observed in this strain likely arise through abnormally high amounts of fission or by inhibited fusion. Mitochondrial fusion and fission are complicated processes involving many proteins and are thought to enable mixing of metabolites and mtDNA thereby allowing optimal mitochondrial function (Cerveny *et al.* 2007; Hoppins *et al.* 2007; Knott and Bossy-Wetzel 2008; Hoppins and Nunnari 2009). Therefore circumstances that disrupt the balance between these opposing forces can be detrimental to the cell. Given that the *mus-10* gene product is a mediator of proteolysis, the altered mitochondrial morphology may result from the accumulation of one or more proteins that promote division or hinder fusion. Indeed, links between E3 ubiquitin ligase complexes and mitochondrial structure have been reported. Mutations in Parkin, an E3 ubiquitin ligase, have been associated with defective mtDNA repair and progression of Parkinson's disease in humans (Dawson 2006; Dodson and Guo 2007). Recent evidence suggests that Parkin functions to promote mitochondrial fission and/or inhibit fusion (Deng *et al.* 2008; Poole *et al.* 2008). In *Saccharomyces cerevisiae*, the F-box protein Mdm30p is involved in ubiquitylation and subsequent degradation of the mitochondrial fusion mediator Fzo1p (Fritz *et al.* 2003; Escobar-Henriques *et al.* 2006; Cohen *et al.* 2008). The *mdm30* mutant was shown to accumulate Fzo1p and exhibit aggregated mitochondria. A physical interaction between Mdm30p and Fzo1p has also been observed (Escobar-Henriques *et al.* 2006). Interestingly, Mdm30p of yeast has a weak homology to *N. crassa* MUS-10, and thus it is tempting to speculate that MUS-10 can interact with FZO-1 and/or other mitochondrial outer membrane proteins. Such an interaction might explain why we observed full-length and truncated forms of MUS-10 in mitochondria upon their overexpression as elevated levels of these proteins may promote binding of MUS-10 to its outer membrane targets. However, we cannot exclude the possibility that MUS-10 is imported into mitochondria and that our detection of the FLAG-tagged MUS-10 proteins in mitochondria stems from increased import arising from high levels of expression. In this case, mitochondrial import would have to rely on internal mitochondrial signal sequences as the N-terminal truncated form of MUS-10 also associated with mitochondria.

There are many unanswered questions regarding the function of MUS-10 and its relationship with mitochondria. However, the *N. crassa mus-10* mutant could provide great insight into the role of ubiquitin-mediated proteolysis in the maintenance of mitochondrial morphology and mtDNA and thus may be used as a model for studying ageing and mitochondrial diseases in humans.

We thank Niji Ohta for her help with our sequencing experiments. We also express our gratitude to Yosuke Morishima and Shigeyuki Kawano who helped photograph mitochondria. This work was funded by grants-in-aid for scientific research 11640619, 08F08756, and 20570001. The Rational Evolutionary Design of Advanced Biomolecules, Saitama Prefecture Collaboration of Regional Entities for the Advancement of Technological Excellence, Japan Science and Technology Agency also supported this work. M.C. was given a grant-in-aid from the Japan Society for the Promotion of Science.

LITERATURE CITED

Akins, R. A., R. L. Kelley and A. M. Lambowitz, 1989 Characterization of mutant mitochondrial plasmids of Neurospora spp. that have incorporated tRNAs by reverse transcription. Mol. Cell. Biol. **9:** 678–691.

Alves, P. C., and A. Videira, 1998 The membrane domain of complex I is not assembled in the stopper mutant E35 of Neurospora. Biochem. Cell. Biol. **76:** 139–143.

Antignani, A., and R. J. Youle, 2006 How do Bax and Bak lead to permeabilization of the outer mitochondrial membrane? Curr. Opin. Cell Biol. **18:** 685–689.

Bai, C., P. Sen, K. Hofmann, L. Ma, M. Goebl *et al.*, 1996 SKP1 connects cell cycle regulators to the ubiquitin proteolysis machinery through a novel motif, the F-box. Cell **86:** 263–274.

Bartlett, K., and S. Eaton, 2004 Mitochondrial beta-oxidation. Eur. J. Biochem. **271:** 462–469.

Bertrand, H., Q. Wu and B. L. Seidel-Rogol, 1993 Hyperactive recombination in the mitochondrial DNA of the natural death nuclear mutant of Neurospora crassa. Mol. Cell. Biol. **13:** 6778–6788.

Boulet, L., G. Karpati and E. A. Shoubridge, 1992 Distribution and threshold expression of the tRNA(Lys) mutation in skeletal muscle of patients with myoclonic epilepsy and ragged-red fibers (MERRF). Am. J. Hum. Genet. **51:** 1187–1200.

Cahan, P., and J. C. Kennell, 2005 Identification and distribution of sequences having similarity to mitochondrial plasmids in mitochondrial genomes of filamentous fungi. Mol. Genet. Genomics **273:** 462–473.

Carroll, A. M., J. A. Sweigard and B. Valent, 1994 Improved vectors for selecting resistance to hygromycin. Fungal Genet. Newsl. **41:** 22.

Cerveny, K. L., Y. Tamura, Z. Zhang, R. E. Jensen and H. Sesaki, 2007 Regulation of mitochondrial fusion and division. Trends Cell Biol. **17:** 563–569.

Chae, M. S., and F. E. Nargang, 2009 Investigation of regulatory factors required for alternative oxidase production in Neurospora crassa. Physiol. Plant **137:** 407–418.

Chatterjee, A., E. Mambo and D. Sidransky, 2006 Mitochondrial DNA mutations in human cancer. Oncogene **25:** 4663–4674.

Chomyn, A., A. Martinuzzi, M. Yoneda, A. Daga, O. Hurko *et al.*, 1992 MELAS mutation in mtDNA binding site for transcription termination factor causes defects in protein synthesis and in respiration but no change in levels of upstream and downstream mature transcripts. Proc. Natl. Acad. Sci. USA **89:** 4221–4225.

Cohen, M. M., G. P. Leboucher, N. Livnat-Levanon, M. H. Glickman and A. M. Weissman, 2008 Ubiquitin-proteasome-dependent degradation of a mitofusin, a critical regulator of mitochondrial fusion. Mol. Biol. Cell **19:** 2457–2464.

Corral-Debrinski, M., T. Horton, M. T. Lott, J. M. Shoffner, M. F. Beal *et al.*, 1992 Mitochondrial DNA deletions in human brain: regional variability and increase with advanced age. Nat. Genet. **2:** 324–329.

Cortopassi, G. A., and N. Arnheim, 1990 Detection of a specific mitochondrial DNA deletion in tissues of older humans. Nucleic Acids Res. **18:** 6927–6933.

Cortopassi, G. A., D. Shibata, N. W. Soong and N. Arnheim, 1992 A pattern of accumulation of a somatic deletion of mitochondrial DNA in aging human tissues. Proc. Natl. Acad. Sci. USA **89:** 7370–7374.

Court, D. A., A. J. Griffiths, S. R. Kraus, P. J. Russell and H. Bertrand, 1991 A new senescence-inducing mitochondrial linear plasmid in field-isolated Neurospora crassa strains from India. Curr. Genet. **19:** 129–137.

d'Alencon, E., A. Taghbalout, C. Bristow, R. Kern, R. Aflalo *et al.*, 2003 Isolation of a new hemimethylated DNA binding protein which regulates dnaA gene expression. J. Bacteriol. **185:** 2967–2971.

D'Souza, A. D., H. Bertrand and R. Maheshwari, 2005 Intramolecular recombination and deletions in mitochondrial DNA of senescent, a nuclear-gene mutant of Neurospora crassa exhibiting "death" phenotype. Fungal Genet. Biol. **42:** 178–190.

Davis, R. H., and F. J. De Serres, 1970 Genetic and microbiological research techniques for Neurospora crassa. Meth. Enzymol. **17A:** 79–143.

Dawson, T. M., 2006 Parkin and defective ubiquitination in Parkinson's disease. J. Neural Transm. **70**(Suppl.): 209–213.

de Serres, F. J., 1980 Mutagenesis at the ad-3A and ad-3B loci in haploid UV-sensitive strains of Neurospora crassa. II. Comparison of dose-response curves for inactivation and mutation induced by UV. Mutat. Res. **71:** 181–191.

de Vries, H., B. Alzner-DeWeerd, C. A. Breitenberger, D. D. Chang, J. C. de Jonge *et al.*, 1986 The E35 stopper mutant of Neurospora crassa: precise localization of deletion endpoints in mitochondrial DNA and evidence that the deleted DNA codes for a subunit of NADH dehydrogenase. EMBO J. **5:** 779–785.

Deng, H., M. W. Dodson, H. Huang and M. Guo, 2008 The Parkinson's disease genes pink1 and parkin promote mitochondrial fission and/or inhibit fusion in Drosophila. Proc. Natl. Acad. Sci. USA **105:** 14503–14508.

Dodson, M. W., and M. Guo, 2007 Pink1, Parkin, DJ-1 and mitochondrial dysfunction in Parkinson's disease. Curr. Opin. Neurobiol. **17:** 331–337.

Escobar-Henriques, M., B. Westermann and T. Langer, 2006 Regulation of mitochondrial fusion by the F-box protein Mdm30 involves proteasome-independent turnover of Fzo1. J. Cell Biol. **173:** 645–650.

Fishel, M. L., Y. R. Seo, M. L. Smith and M. R. Kelley, 2003 Imbalancing the DNA base excision repair pathway in the mitochondria; targeting and overexpressing N-methylpurine DNA glycosylase in mitochondria leads to enhanced cell killing. Cancer Res. **63:** 608–615.

Freitag, M., P. C. Hickey, N. B. Raju, E. U. Selker and N. D. Read, 2004 GFP as a tool to analyze the organization, dynamics and function of nuclei and microtubules in Neurospora crassa. Fungal Genet. Biol. **41:** 897–910.

Fritz, S., N. Weinbach and B. Westermann, 2003 Mdm30 is an F-box protein required for maintenance of fusion-competent mitochondria in yeast. Mol. Biol. Cell. **14:** 2303–2313.

Fukui, H., and C. T. Moraes, 2009 Mechanisms of formation and accumulation of mitochondrial DNA deletions in aging neurons. Hum. Mol. Genet. **18:** 1028–1036.

Galagan, J. E., S. E. Calvo, K. A. Borkovich, E. U. Selker, N. D. Read *et al.*, 2003 The genome sequence of the filamentous fungus Neurospora crassa. Nature **422:** 859–868.

Gerber, J., and R. Lill, 2002 Biogenesis of iron-sulfur proteins in eukaryotes: components, mechanism and pathology. Mitochondrion **2:** 71–86.

Good, A. G., and W. L. Crosby, 1989 Anaerobic induction of alanine aminotransferase in barley root tissue. Plant Physiol. **90:** 1305–1309.

Green, D. R., 2005 Apoptotic pathways: ten minutes to dead. Cell **121:** 671–674.

Gunter, T. E., D. I. Yule, K. K. Gunter, R. A. Eliseev and J. D. Salter, 2004 Calcium and mitochondria. FEBS Lett. **567:** 96–102.

Handa, N., Y. Noguchi, Y. Sakuraba, P. Ballario, G. Macino *et al.*, 2000 Characterization of the Neurospora crassa mus-25 mutant: the gene encodes a protein which is homologous to the Saccharomyces cerevisiae Rad54 protein. Mol. Gen. Genet. **264:** 154–163.

Hanway, D., J. K. Chin, G. Xia, G. Oshiro, E. A. Winzeler *et al.*, 2002 Previously uncharacterized genes in the UV- and MMS-induced DNA damage response in yeast. Proc. Natl. Acad. Sci. USA **99:** 10605–10610.

Hausner, G., K. A. Nummy, S. Stoltzner, S. K. Hubert and H. Bertrand, 2006 Biogenesis and replication of small plasmid-like derivatives of the mitochondrial DNA in Neurospora crassa. Fungal Genet. Biol. **43:** 75–89.

Higuchi, M., 2007 Regulation of mitochondrial DNA content and cancer. Mitochondrion **7:** 53–57.

Ho, M. S., C. Ou, Y. R. Chan, C. T. Chien and H. Pi, 2008 The utility F-box for protein destruction. Cell. Mol. Life Sci. **65:** 1977–2000.

Hoppins, S., and J. Nunnari, 2009 The molecular mechanism of mitochondrial fusion. Biochim. Biophys. Acta **1793:** 20–26.

Hoppins, S., L. Lackner and J. Nunnari, 2007 The machines that divide and fuse mitochondria. Annu. Rev. Biochem. **76:** 751–780.

Jackson, P. K., and A. G. Eldridge, 2002 The SCF ubiquitin ligase: an extended look. Mol. Cell **9:** 923–925.

Kafer, E., 1981 Mutagen sensitivities and mutator effects of MMS-sensitive mutants in Neurospora. Mutat. Res. **80:** 43–64.

Kafer, E., 1983 Epistatic grouping of repair-deficient mutants in Neurospora: comparative analysis of two uvs-3 alleles, uvs-6 and their mus double mutant strains. Genetics **105:** 19–33.

Kafer, E., and E. Perlmutter, 1980 Isolation and genetic analysis of MMS-sensitive mus mutants of neurospora. Can. J. Genet. Cytol. **22:** 535–552.

Kelkar, H. S., J. Griffith, M. E. Case, S. F. Covert, R. D. Hall *et al.*, 2001 The Neurospora crassa genome: cosmid libraries sorted by chromosome. Genetics **157:** 979–990.

Knott, A. B., and E. Bossy-Wetzel, 2008 Impairing the mitochondrial fission and fusion balance: a new mechanism of neurodegeneration. Ann. N Y Acad. Sci. **1147:** 283–292.

Kothe, G. O., M. Kitamura, M. Masutani, E. U. Selker and H. Inoue, 2010 PARP is involved in replicative aging in Neurospora crassa. Fungal Genet. Biol. **47:** 297–309.

Krishnan, K. J., A. K. Reeve and D. M. Turnbull, 2007 Do mitochondrial DNA mutations have a role in neurodegenerative disease? Biochem. Soc. Trans. **35:** 1232–1235.

Laemmli, U. K., 1970 Cleavage of structural proteins during the assembly of the head of bacteriophage T4. Nature **227:** 680–685.

Lambowitz, A. M., 1979 Preparation and analysis of mitochondrial ribosomes. Methods Enzymol. **59:** 421–433.

Lill, R., and U. Muhlenhoff, 2005 Iron-sulfur-protein biogenesis in eukaryotes. Trends Biochem. Sci. **30:** 133–141.

Maheshwari, R., and A. Navaraj, 2008 Senescence in fungi: the view from Neurospora. FEMS Microbiol. Lett. **280:** 135–143.

Myers, C. J., A. J. Griffiths and H. Bertrand, 1989 Linear kalilo DNA is a Neurospora mitochondrial plasmid that integrates into the mitochondrial DNA. Mol. Gen. Genet. **220:** 113–120.

Nargang, F. E., J. B. Bell, L. L. Stohl and A. M. Lambowitz, 1983 A family of repetitive palindromic sequences found in Neurospora mitochondrial DNA is also found in a mitochondrial plasmid DNA. J. Biol. Chem. **258:** 4257–4260.

Navaraj, A., A. Pandit and R. Maheshwari, 2000 Senescent: a new Neurospora crassa nuclear gene mutant derived from nature exhibits mitochondrial abnormalities and a "death" phenotype. Fungal Genet. Biol. **29:** 165–173.

Newmeyer, D., and D. R. Galeazzi, 1978 A meiotic UV-sensitive mutant that causes deletion of duplications in Neurospora. Genetics **89:** 245–269.

Newmeyer, D., A. L. Schroeder and D. R. Galeazzi, 1978 An apparent connection between histidine, recombination, and repair in Neurospora. Genetics **89:** 271–279.

Niagro, F. D., and N. C. Mishra, 1989 An ethidium bromide induced mutant of Neurospora crassa defective in mitochondrial DNA. Curr. Genet. **16:** 303–305.

Niagro, F. D., and N. C. Mishra, 1990 Biochemical, genetic and ultrastructural defects in a mitochondrial mutant (ER-3) of Neurospora crassa with senescence phenotype. Mech. Ageing Dev. **55:** 15–37.

Ninomiya, Y., K. Suzuki, C. Ishii and H. Inoue, 2004 Highly efficient gene replacements in Neurospora strains deficient for nonhomologous end-joining. Proc. Natl. Acad. Sci. USA **101:** 12248–12253.

Orbach, M. J., 1994 A cosmid with a HyR marker for fungal library construction and screening. Gene **150:** 159–162.

Perkins, D. D., J. A. Kinsey, D. K. Asch and G. D. Frederick, 1993 Chromosome rearrangements recovered following transformation of Neurospora crassa. Genetics **134:** 729–736.

Poole, A. C., R. E. Thomas, L. A. Andrews, H. M. McBride, A. J. Whitworth *et al.*, 2008 The PINK1/Parkin pathway regulates mitochondrial morphology. Proc. Natl. Acad. Sci. USA **105:** 1638–1643.

Reeve, A. K., K. J. Krishnan and D. Turnbull, 2008 Mitochondrial DNA mutations in disease, aging, and neurodegeneration. Ann. N Y Acad. Sci. **1147:** 21–29.

Rimessi, A., C. Giorgi, P. Pinton and R. Rizzuto, 2008 The versatility of mitochondrial calcium signals: from stimulation of cell metabolism to induction of cell death. Biochim. Biophys. Acta **1777:** 808–816.

Rouault, T. A., and W. H. Tong, 2005 Iron-sulphur cluster biogenesis and mitochondrial iron homeostasis. Nat. Rev. Mol. Cell. Biol. **6:** 345–351.

Rowley, N., C. Prip-Buus, B. Westermann, C. Brown, E. Schwarz *et al.*, 1994 Mdj1p, a novel chaperone of the DnaJ family, is involved in mitochondrial biogenesis and protein folding. Cell **77:** 249–259.

Ryan, F. J., G. W. Beadle and E. L. Tatum, 1943 The tube method of measuring the growth rate of Neurospora. Am. J. Bot. **30:** 784–799.

Sakuraba, Y., A. L. Schroeder, C. Ishii and H. Inoue, 2000 A Neurospora double-strand-break repair gene, mus-11, encodes a RAD52 homologue and is inducible by mutagens. Mol. Gen. Genet. **264:** 392–401.

Schroeder, A. L., 1970 Ultraviolet-sensitive mutants of Neurospora. I. Genetic basis and effect on recombination. Mol. Gen. Genet. **107:** 291–304.

Schroeder, A. L., 1986 Chromosome instability in mutagen sensitive mutants of Neurospora. Curr. Genet. **10:** 381–387.

Sciacco, M., E. Bonilla, E. A. Schon, S. DiMauro and C. T. Moraes, 1994 Distribution of wild-type and common deletion forms of mtDNA in normal and respiration-deficient muscle fibers from patients with mitochondrial myopathy. Hum. Mol. Genet. **3:** 13–19.

Seidel-Rogol, B. L., J. King and H. Bertrand, 1989 Unstable mitochondrial DNA in natural-death nuclear mutants of Neurospora crassa. Mol. Cell. Biol. **9:** 4259–4264.

Sheng, T. C., 1951 A gene that causes natural death in Neurospora crassa. Genetics **36:** 199–212.

Simonetti, S., X. Chen, S. DiMauro and E. A. Schon, 1992 Accumulation of deletions in human mitochondrial DNA during normal aging: analysis by quantitative PCR. Biochim. Biophys. Acta **1180:** 113–122.

Sizemore, S. T., and J. V. Paietta, 2002 Cloning and characterization of scon-3+, a new member of the Neurospora crassa sulfur regulatory system. Eukaryot. Cell **1:** 875–883.

Tamaru, H., and H. Inoue, 1989 Isolation and characterization of a laccase-derepressed mutant of Neurospora crassa. J. Bacteriol. **171:** 6288–6293.

Watanabe, K., Y. Sakuraba and H. Inoue, 1997 Genetic and molecular characterization of Neurospora crassa mus-23: a gene involved in recombinational repair. Mol. Gen. Genet. **256:** 436–445.

Willems, A. R., M. Schwab and M. Tyers, 2004 A hitchhiker's guide to the cullin ubiquitin ligases: SCF and its kin. Biochim. Biophys. Acta **1695:** 133–170.

Xu, G., and Y. Shi, 2007 Apoptosis signaling pathways and lymphocyte homeostasis. Cell Res. **17:** 759–771.

Yin, S., J. Heckman and U. L. RajBhandary, 1981 Highly conserved GC-rich palindromic DNA sequences flank tRNA genes in Neurospora crassa mitochondria. Cell **26:** 325–332.

Zheng, L., V. L. Cash, D. H. Flint and D. R. Dean, 1998 Assembly of iron-sulfur clusters. Identification of an iscSUA-hscBA-fdx gene cluster from Azotobacter vinelandii. J. Biol. Chem. **273:** 13264–13272.

Communicating editor: E. U. Selker